Chapter 4

A Comparative Study on Some Fault Diagnosis Techniques in Three-Phase Inverter Fed Induction Motors

Bilal Djamal Eddine Cherif, Azeddine Bendiabdellah, Mokhtar Bendjebbar and Laribi Souad

Additional information is available at the end of the chapter

http://dx.doi.org/10.5772/intechopen.79960

Abstract

The growing importance of power conversion systems and their dependency on the performance and reliability of static converters has motivated extensive research efforts in this field. A variety of different techniques have been applied to detect open-circuit faults in power converters. The present chapter is focusing on the techniques of detection and localization of open-circuit faults in a three phase voltage source inverter fed induction motor. A comparative study is carried out between different detection techniques: the Park current vectors and its enhancement by using the polar coordinates, the mean value of the currents, the stator current spectrum analysis and the measurement of the current drop. The aim of this comparison is to investigate the relative strengths and weaknesses of the different techniques and evaluate the performance of each detection technique studied. The comparison study focuses on the time detection, the localization ability and the hardware aspect. To validate these techniques, an experimental setup is developed in our diagnostic group laboratory which consists of a two-level voltage source inverter controlled by a *DSPACE-1104*, Card to generate the PWM vector control of the induction motor. The obtained simulation and experimental results illustrate well the detection feasibility of each technique as well as the benefits and merits of the performed comparative study.

Keywords: induction motor, inverter, open-circuit fault, detection, localization, Park's vectors, polar coordinates, mean value, frequency spectrum, current drop

1. Introduction

The applications of electronics were for a long time limited to the technique of high frequencies. The possibilities of application were limited by the unreliability of the electronic elements available at that time. This reliability was insufficient to meet the high demands of new applications in the industrial field. It was only after the development of special electronic power components of higher reliability and more limited tolerance that new techniques could be envisaged, thus creating a new branch of electronics called power electronics.

One area where power electronics is widely used today is the industrial applications related to machine-static power converter associations, particularly the industrial variable speed AC drives. These drives are mainly used in which the machines are connected through a static power electronic converter usually a three-phase inverter. It is estimated that about 38% of the faults in these industrial drives are due to failures of the supply system. Some uses of the machine-static power converter sets do not tolerate untimely failures, mechanical or electrical failures at the machine or related to static power converter failure. An industrial survey [1] conducted in 2011, comes to the conclusion that 93% of respondents stated that reliability is a paramount issue in the field of static power electronic converters. The faults of the static power converters have various causes; they can be related to the open-circuit faults of the IGBT switches for example. This type of malfunction induces damage constraints for the production system if the personnel are not notified and a nuisance shutdown can eventually result.

The growing interest of manufacturers in the maintenance of electrical drives justifies the emphasis placed on research into the diagnosis of machine-static power converter associations. The complexity of the systems involved and the necessary approach from the new angle of diagnosis today require a preliminary work of detection/diagnosis of the faults of the machine-converter association.

Several researchers have studied the behavior of static power converters with internal failure, focusing particularly on the open-circuit fault of an IGBT switch. Such a fault can lead to secondary faults in other converter components that can result in high repair costs [2].

Authors [3, 4] propose the Park vector technique, the principle of this technique is based on the tracking of the current trajectory of Park (i_d, i_q). In the healthy case, the trajectory takes a circle shape and in the case of an IGBT switch open-circuit fault, the circle becomes a semicircle.

The position of this trajectory in the *(d-q)* frame makes it possible to calculate the intervals of the angles of the fault to localize the faulty IGBT. Other researchers [5–8] have proposed the Park.

Average current (i_{dmean}, i_{qmean}) technique to calculate the exact open-circuit fault angle in order to identify the faulty IGBT switch. Authors [9–11] have proposed the technique based on the spectral analysis of the stator currents. This technique is based on the study of the harmonic analysis of each phase current. The amplitude and argument of each harmonic can be used in detecting and localizing the faults. The analysis of the first harmonics shows that the difference between the healthy state and the open-circuit fault case resides in the zero-order harmonics which signifies the presence of the DC component in the signal. The argument of

http://dx.doi.org/10.5772/intechopen.79960

the harmonic zero with respect to the fundamental makes it possible to know the type of fault; on the other hand, the argument of this harmonic also makes it possible to know the faulty IGBT switch either the high or the lower one. The authors [12] combined normalized standard currents with additional diagnostic variables for one or more IGBT switch open-circuit faults. The diagnostic alarms were performed by the Boolean output signals. In the paper presented by [13], the same authors proposed another extension based on the use of fuzzy logic symptoms. The author [14] proposes the Clarke technique followed by the polarity of the trajectory slope in the complex α-β frame identify the faulty IGBT switch.

The present chapter is focusing on techniques of detection and localization of IGBT switch open-circuit faults in a three phase voltage source inverter fed induction motor. A comparative study is carried out between different detection techniques: the Park current vectors and its enhancement by using the polar coordinates, the mean value of the currents, the stator current spectrum analysis and the measurement of the current drop. The comparison study aims at exhibiting the relative strengths and weaknesses of the different techniques and at assessing each detection technique in terms of its performance; that is the time detection and the localization ability; as well as in terms of hardware; that is the number of current sensors required for IGBT switch open-circuit fault detection. To validate these techniques, an experimental setup is developed in our diagnostic group laboratory which consists of a two-level voltage source inverter controlled by a *DSPACE-1104* Card to generate the *PWM* vector control of the induction motor. The obtained simulation and experimental results illustrate well the detection feasibility of each technique as well as the benefits and merits of the performed comparative study.

2. Space voltage vector and switching states for the case of both healthy and faulty inverter

Figure 1 shows the general structure of a three phase two-level voltage source inverter feeding an induction motor.

This inverter is controlled by the *PWM* vector control strategy. For each leg of the inverter, there are two possible states:

State 1: The higher switch *Kx* (*x = 1, 2 or 3*) is closed, while the lower switch K_2x (*x = 1, 2 or 3*) is open. The output voltage relative to the neutral of the dc source is V_{dc}.

State 0: The lower switch *Kx* (*x = 1, 2 or 3*) is closed, while the higher switch K_1x (*x = 1, 2 or 3*) is open. The output voltage relative to the neutral of the dc source is *0v*.

It is to note that the faulty inverter used in this chapter is defined as an inverter with one of its IGBT switch exhibiting an open-circuit fault.

The experimental setup used in this chapter is depicted in the photo of **Figure 2**. It includes a three-phase squirrel-cage induction motor fed by a three-phase two-level voltage source inverter.

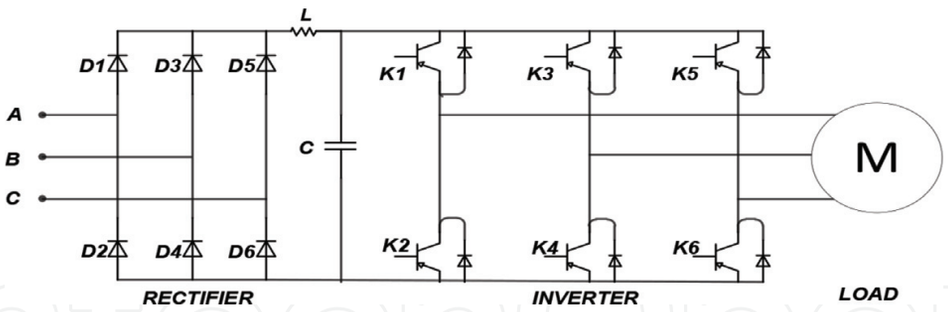

Figure 1. The structure of a three phase two-level inverter.

Figure 2. Experimental setup.

The detailed characteristics of the motor are given in the appendix. Furthermore, the motor is mechanically coupled to a DC generator supplying a bank of resistors which allows varying the load torque. Moreover, the measuring system includes three current Hall Effect sensors and three voltage sensors and a DSPACE 1104 acquisition card to generate pulses for triggering the IGBT's gates in the inverter. The whole set is connected to a computer for visualizing and analyzing the processed sensed signal [14].

Because of the randomness of the measured signals and for a reliable analysis, 05 acquisitions are performed for each case. The acquisition time used is T_{acq} = 20s. To study the effect of the load on the induction motor signals, the following mode of operation is considered; the rated load operation with a rated current of 7A and an estimated torque of 20 Nm and a frequency of sampling Fe = 1.5kHz.

3. Fault detection techniques for a faulty inverter

During its operation, the inverter is subjected to various internal and external constraints resulting in its failure; especially those failures related to the IGBT semiconductor switches because of their fragility. Two types of faults are usually linked with the inverter and can be reported in **Table 1** as follows:

Faults	Description
Short-circuit	Short-circuit faults affecting the IGBT switches are the most serious faults. In the presence of such a fault, the current reaches limits which can cause the fusion of its chip or its connection. If the detection of this type of fault does not occur rapidly (less than 10 μs), then the IGBT switch which is still active on the same leg undergoes the same phenomenon and so the whole inverter leg is shorted.
Open-circuit	Open-circuit faults affecting the IGBT switches may occur when, for any reason, the IGBT is disconnected, is damaged, or had a problem in its grid control signal. This type of fault is very difficult to perceive directly because the motor can continue to operate but with a degradation of its performance due to the occurrence of fluctuations in the mechanical parameters (speed and torque) as well as an imbalance of the currents where the currents of the other two healthy legs take high values to maintain the average torque and the speed. The starting of the motor in the presence of this type of fault cannot always be ensured.

Table 1. Description of inverter faults.

Number	Methods for open-circuit IGBT switch faults
1	Technique based on the Park vectors and enhanced Park vectors with polar coordinates
2	Technique based on the mean value of the currents
3	Technique based on the stator current spectrum analysis
4	Technique based on the measure of the current drop

Table 2. Fault diagnosis used techniques.

In this chapter section, different techniques for fault detection and localization of the inverter IGBT switches open-circuit fault are presented in the summarized **Table 2** and thoroughly discussed.

3.1. Technique based on the Park vectors

The Park vectors technique is based on the tracking of the trajectory of the current vector. Indeed, in normal conditions (without fault), the trajectory of the current vector in the *d-q* frame is a circle. The circle becomes a semicircle when an IGBT open-circuit fault of an inverter leg occurs. The position of this semicircle in the *d-q* frame allows identifying the faulty switch as developed by [10]. Applying the Park transformation on the three phase currents (i_a, i_b, i_c) results in two currents (i_d, i_q) in the *d-q* frame. The current is expressed by the following mathematical system:

$$\begin{cases} i_{ds} = \frac{2}{3} i_{as} - \frac{1}{3} i_{bs} - \frac{1}{3} i_{cs} \\ i_{qs} = \frac{1}{\sqrt{3}} (i_{bs} - i_{cs}) \end{cases} \quad (1)$$

Its slope is used to identify the faulty leg. As mentioned above, the extraction of information of any faulty leg can be obtained from the angle between the current vector and the *d-q* frame using the following equation:

$$\theta_l = \arctan\left(\frac{i_{qs}}{i_{ds}}\right) \quad (2)$$

where θ_l is the inverter leg fault angle.

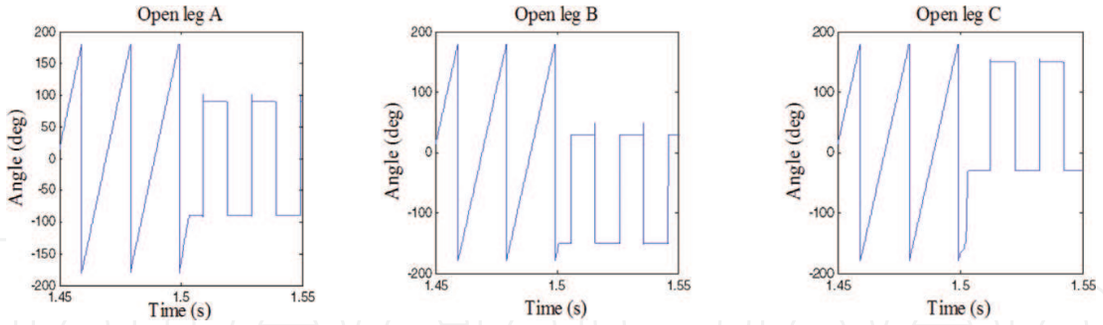

Figure 3. Ideal shapes of the leg fault angle θ_l (simulation results).

Figure 3 depicts the angle of the faulty leg when applying an open-circuit fault at $t = 1.5\ s$.

In reference to **Figure 3**, the leg fault angle θ_l is used to identify the faulty leg of the inverter. For the case of a healthy inverter, the angle values are always π or -π. Any angle values different from π or -π are therefore considered as an indication confirming faulty legs presence. The various faulty inverter legs corresponding to the various fault angle values are expressed in **Table 3**.

The Park trajectory slope is used to identify the faulty switch. As mentioned above, the extraction of information of any faulty switch can be obtained from the angle between the mean current vector and the *d-q* frame using the following equation:

$$\theta_K = \arctan\left(i_{qsmean} / i_{dsmean}\right) \tag{3}$$

where θ_K is the inverter switch fault angle.

Figure 4 depicts the angle of the faulty switch when applying an open-circuit fault at $t = 1.5$ s.

Figure 4 shows the fault angles switch θ_K. The various faulty inverter switches corresponding to the various fault angle values are expressed in **Table 4**.

For example for the case of a faulty inverter switch K_1 corresponds the angle intervals $[0, \pi/2]$ or $[3\pi/2, 2\pi]$.

Figure 5 depicts the trajectories of the currents for both healthy and faulty inverters.

Faulty leg	IGBT switches	Leg fault angle θ_l
leg A	K_1, K_2	$\pi/2$ *or* $-\pi/2$
leg B	K_3, K_4	$5\pi/6$ *or* $-\pi/6$
leg C	K_5, K_6	$5\pi/6$ *or* $-\pi/6$

Table 3. Current vector position as function of θ_l.

http://dx.doi.org/10.5772/intechopen.79960

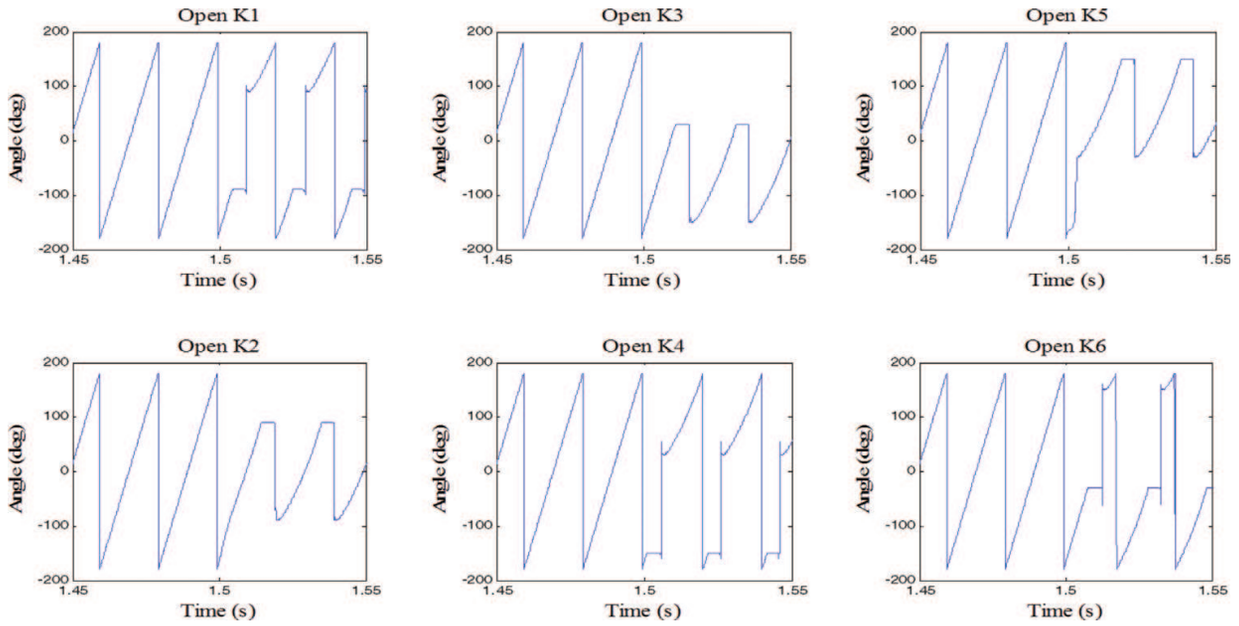

Figure 4. Ideal shapes of the IGBT switch open-circuit fault angle θ_K (simulation result).

IGBT	**Fault angles of inverter switch θ_K**
K_1 open	*[0, π/2] or [3π/2, 2π]*
K_2 open	*[π/2, 3π/2]*
K_3 open	*[π/6, 7π/6]*
K_4 open	*[0, π/6] or [7π/6, 2π]*
K_5 open	*[5π/6, 11π/6]*
K_6 open	*[0, 5π/6] or [11π/6, 2π]*

Table 4. Open-circuit switch fault angles.

3.1.1. Enhanced Park vectors with polar coordinates

A polar coordinates calculation is proposed associated with the technique of Park vectors in order to enhance the inverter IGBT switch fault localization. This section focuses on the localization of each faulty IGBT switch by calculating the borders of each trajectory as well as the fault current vector. This calculation is carried out by proposing the use of the polar coordinates diagram as shown by **Figure 6**.

The mathematical model based on the polar coordinates is related to the trajectory and the angle θ_{icf} of the specified faulty IGBT. Consequently, a change in the shape of the trajectory and the angle indicates the occurrence of a fault condition. This represents an indicator for the localization of the faulty IGBT switch. The angle is calculated from Eqs. 4–6 as follows:

$$\theta_{icf} = \sum_{i=0}^{N} \pi r^2 \rho / 360 \tag{4}$$

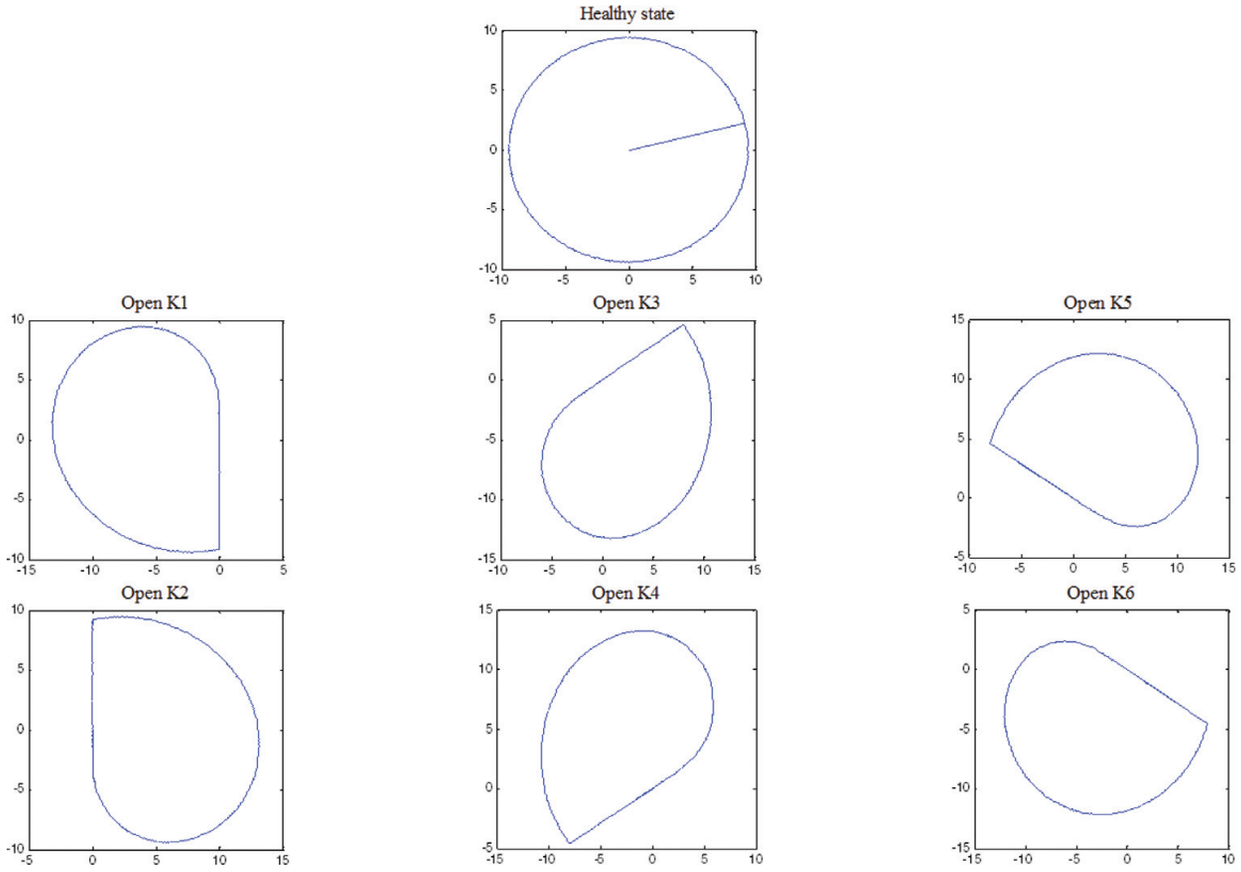

Figure 5. Currents trajectories of healthy and faulty inverter (simulation results).

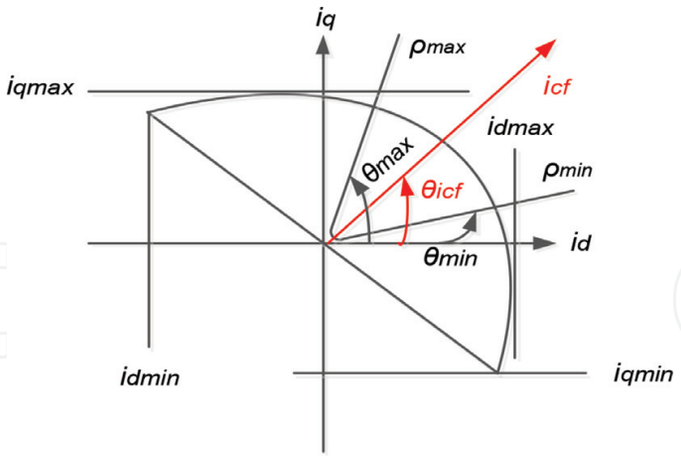

Figure 6. Proposed schematic geometry of polar coordinates.

The radius of this trajectory can be calculated from the following equation:

$$r=\sqrt{i_{ds}{}^2+i_{qs}{}^2} \tag{5}$$

$$\rho=\rho_{max}-\rho_{min} \tag{6}$$

http://dx.doi.org/10.5772/intechopen.79960

IGBT	*Fault current vector i_{cf}*
K_1 open	$i_{cf} = 6.5\angle\pi$
K_2 open	$i_{cf} = 6.5\angle 2\pi$
K_3 open	$i_{cf} = 4.95\angle 5\pi/3$
K_4 open	$i_{cf} = 4.95\angle 2\pi/3$
K_5 open	$i_{cf} = 5.3\angle\pi/3$
K_6 open	$i_{cf} = 5.3\angle 4\pi/3$

Table 5. Fault current vector for each faulty switch.

The *d-q* currents at the center of the trajectory i_{dc} and i_{qc} can be computed using the maximum and minimum of the currents vectors as follows:

$$\begin{cases} \boldsymbol{i_{dsc}} = \frac{1}{2}(\boldsymbol{i_{dsmax}} + \boldsymbol{i_{dsmin}}) \\ \boldsymbol{i_{qsc}} = \frac{1}{2}(\boldsymbol{i_{qsmax}} + \boldsymbol{i_{qsmin}}) \end{cases} \tag{7}$$

For the case of a faulty IGBT switch, the current vector is given by the following equation:

$$\boldsymbol{i_{cf}} = \boldsymbol{i_{dsc}} + j\boldsymbol{i_{qsc}} \tag{8}$$

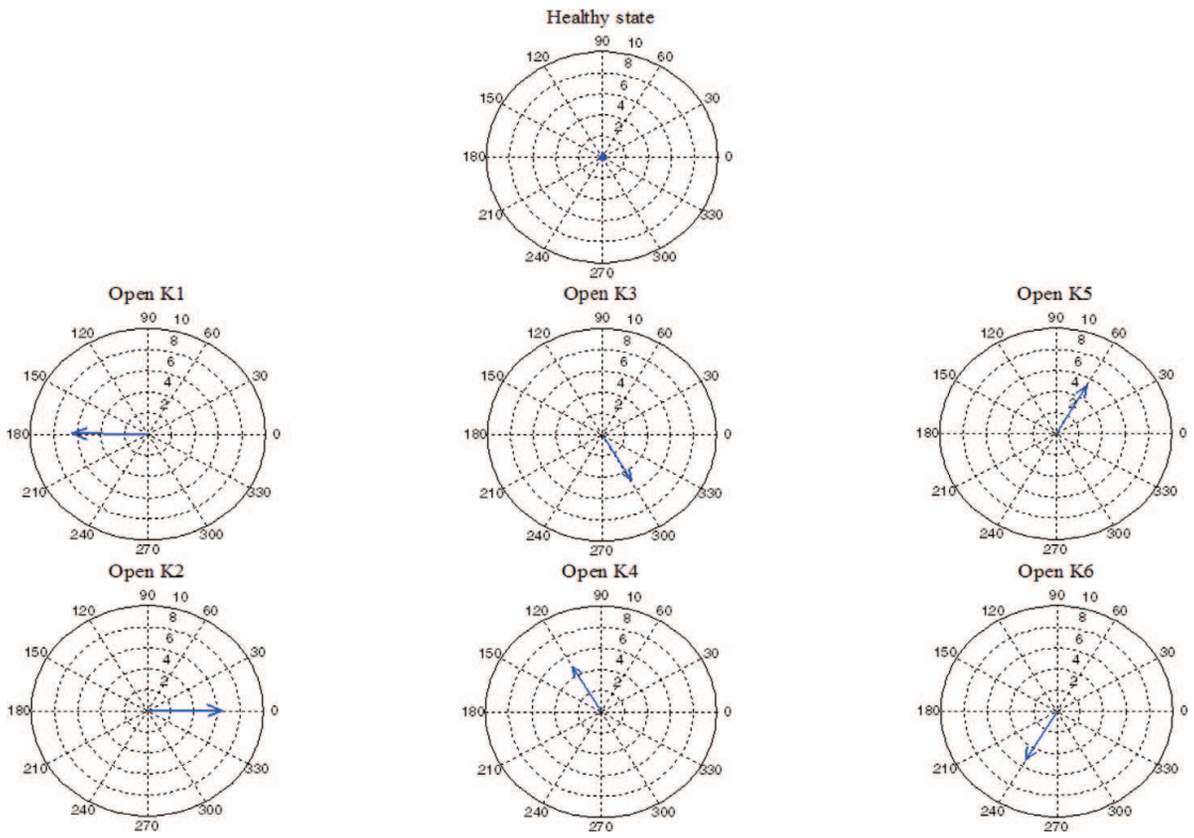

Figure 7. Graphical representation of fault current vectors (simulation results).

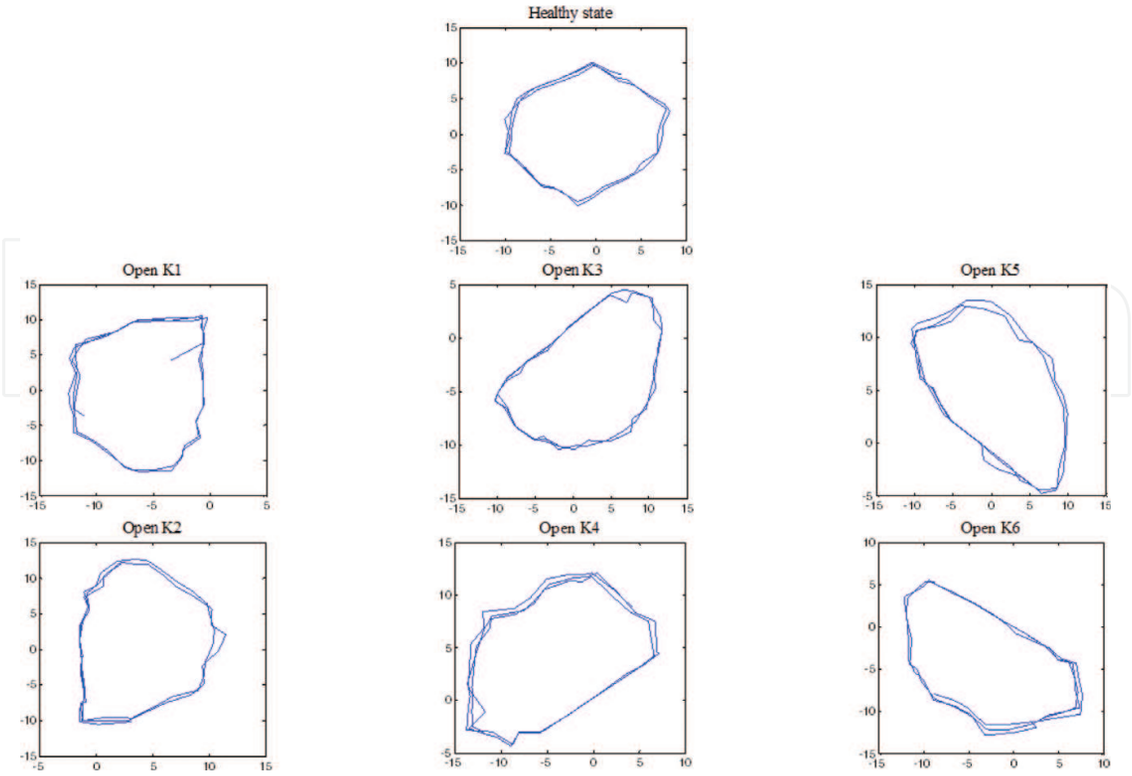

Figure 8. Currents trajectories of healthy and faulty inverter (experimental result).

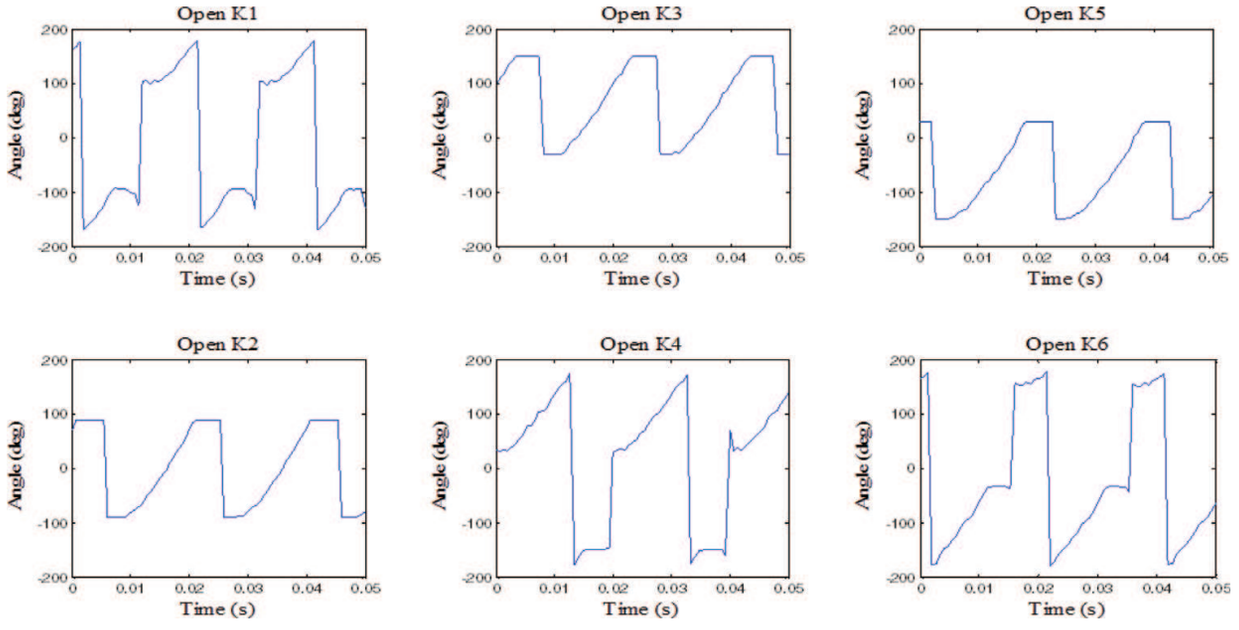

Figure 9. Ideal shapes of the IGBT switch open-circuit fault angle θ_K (experimental results).

From this calculation, the open-circuit fault of each IGBT switch can be localized and **Table 5** summarizes the computation of the fault angle values and the fault current vectors for the case of each faulty IGBT switch.

http://dx.doi.org/10.5772/intechopen.79960

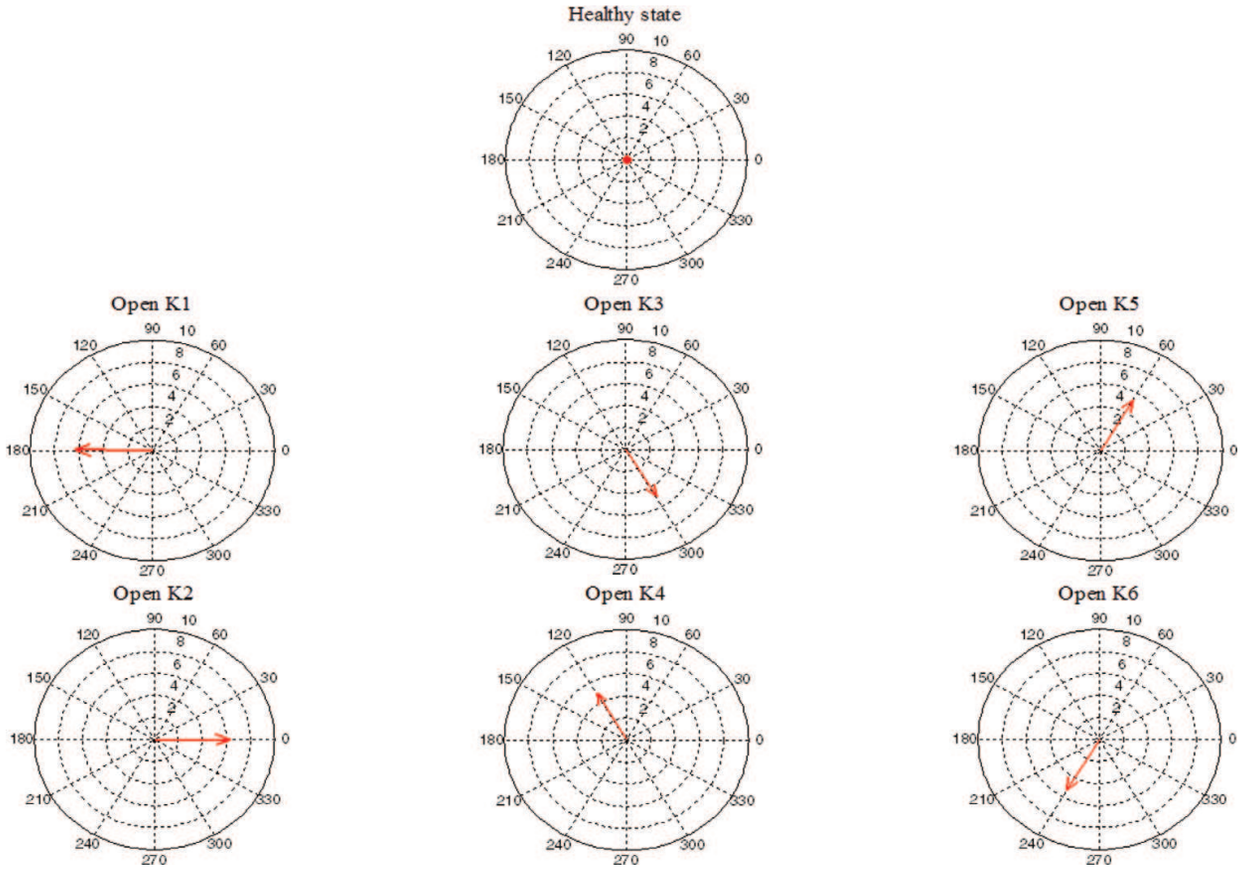

Figure 10. Graphical representation of fault current vectors (experimental results).

A significant advantage of the polar coordinates calculation is that it enables to yield the exact value of the angle for inverter faults detection while other existing techniques gives rather an interval of angles.

Figure 7 shows the fault current vector i_{cf} when the inverter is operating under both healthy and faulty conditions. For the case of a healthy inverter, the average amplitude of the fault current vector is zero. If a failure occurs, the magnitude of the fault current vector becomes non-zero. The faulty IGBT is identified by the phase angle and the fault current vector magnitude.

3.1.2. Experimental results for healthy and faulty inverters using the Park vectors technique with polar coordinates

See **Figures 8–10**.

4. Technique based on the mean value of the currents

This technique uses the mean phase current value for fault detection. A fault in a semiconductor switch can produce offsets in the currents of the electrical machine phases. This diagnostic

technique is to calculate the mean values of these currents from which the fault can be detected. A current threshold is defined in order to distinguish between the open-circuit faults in a semiconductor switch.

The mathematical model of this technique is illustrated by the following steps:

1st step: Extraction of the three currents of the stator (i_{as}, i_{bs}, i_{cs}) as follows:

$$\begin{cases} I_{as} = 0 \\ I_{bs} = I\cos\left(\omega t + \varphi - \dfrac{2\pi}{3}\right) \\ I_{cs} = I\cos\left(\omega t + \varphi - \dfrac{4\pi}{3}\right) \end{cases} \tag{9}$$

2nd step: Calculation of the mean value of the three stator currents:

$$\begin{cases} I_{amean} = sum\left({}^{I_{as}}/_{length(i_a)}\right) \\ I_{bmean} = sum\left({}^{I_{bs}}/_{length(i_b)}\right) \\ I_{cmean} = sum\left({}^{I_{cs}}/_{length(i_c)}\right) \end{cases} \tag{10}$$

where length (Ia,b,c): number of point the three current signals *Ia, Ib, Ic.*

After the introduction of a fault in the IGBT of the inverter, one can easily observe the change in the form of the stator currents and also their mean values. This technique allows us therefore to easily identify and localize the faults which are expressed by the following equation:

$$I_{mean} = {}^{(I_{amean}+I_{bmean}+I_{cmean})}/_{3} \tag{11}$$

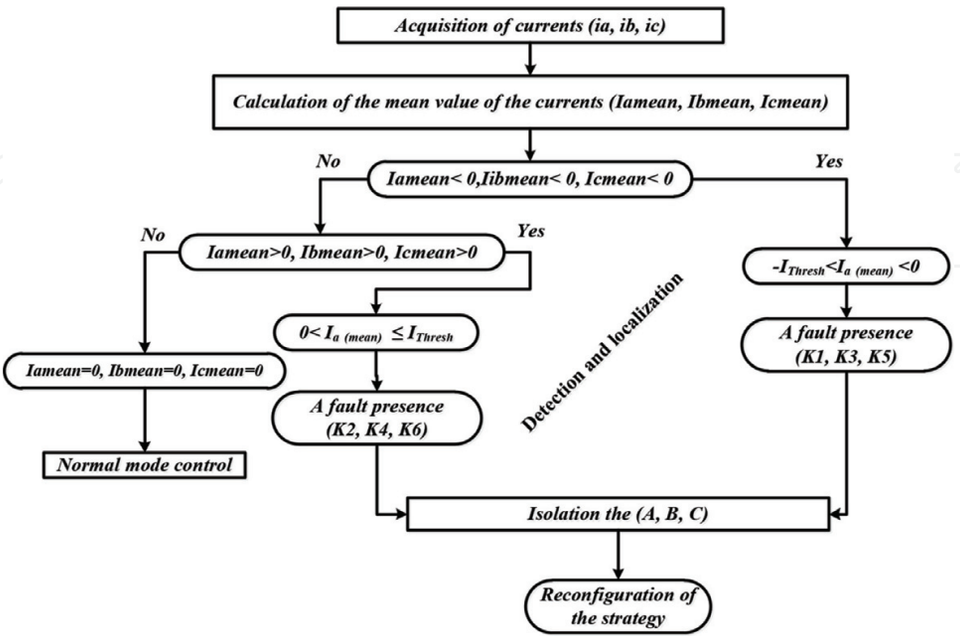

Figure 11. Detection algorithm of faulty inverter using the mean value of stator currents technique.

http://dx.doi.org/10.5772/intechopen.79960

State	Phase *A*	Phase *B*	Phase *C*
Healthy	I_{Thresh}, (I_{Thresh} =0)	I_{Thresh}, (I_{Thresh} =0)	I_{Thresh}, (I_{Thresh} =0)
K_1 open	$-I_{Thresh} < I_{amean} < 0$, ($I_{amean} = -1.5$)	$I_{bmean} \geq 0$, ($I_{bmean} = 0$)	$I_{cmean} \geq 0$, ($I_{cmean} = 0$)
K_3 open	$I_{amean} \geq 0$, ($I_{amean} = 0$)	$-I_{Thresh} < I_{bmean} < 0$, ($I_{bmean} = -1.5$)	$I_{cmean} \geq 0$, ($I_{cmean} = 0$)
K_5 open	$I_{amean} \geq 0$, ($I_{amean} = 0$)	$I_{bmean} \geq 0$, ($I_{bmean} = 0$)	$-I_{Thresh} < I_{cmean} < 0$, ($I_{cmean} = -1.5$)
K_2 open	$0 < I_{amean} \leq I_{Thresh}$, ($I_{amean} = 1.5$)	$I_{bmean} \leq 0$, ($I_{bmean} = 0$)	$I_{cmean} \leq 0$, ($I_{cmean} = 0$)
K_4 open	$I_{amean} \leq 0$, ($I_{amean} = 0$)	$0 < I_{bmean} \leq I_{Thresh}$, ($I_{bmean} = 1.5$)	$I_{cmean} \leq 0$, ($I_{cmean} = 0$)
K_6 open	$I_{amean} \leq 0$, ($I_{amean} = 0$)	$I_{bmean} \leq 0$, ($I_{bmean} = 0$)	$0 < I_{cmean} \leq I_{Thresh}$, ($I_{cmean} = 1.5$)

Table 6. Characteristics of various types of fault of the inverter.

The open-circuit fault detection algorithm that will be applied in this technique is based on the calculated mean value of the currents and can be described by the following algorithm as shown in **Figure 11** (**Table 6**).

4.1. Simulation results for healthy and faulty inverter using the technique of the mean value of the currents

See **Figures 12** and **13**.

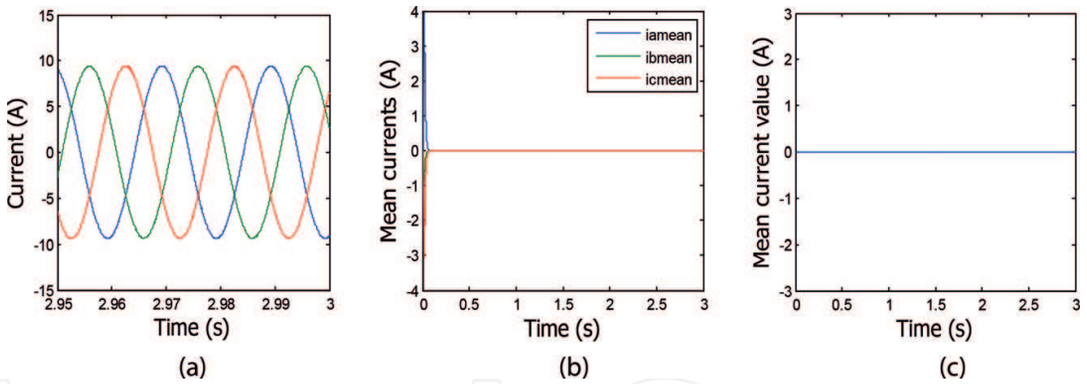

Figure 12. Current characteristics for a healthy inverter (simulation results). (a) Three stator currents (I_a, I_b, I_c), (b) Mean values of three stator currents (I_{amean}, I_{bmean}, I_{cmean}), (c) Mean value of current I_{mean}.

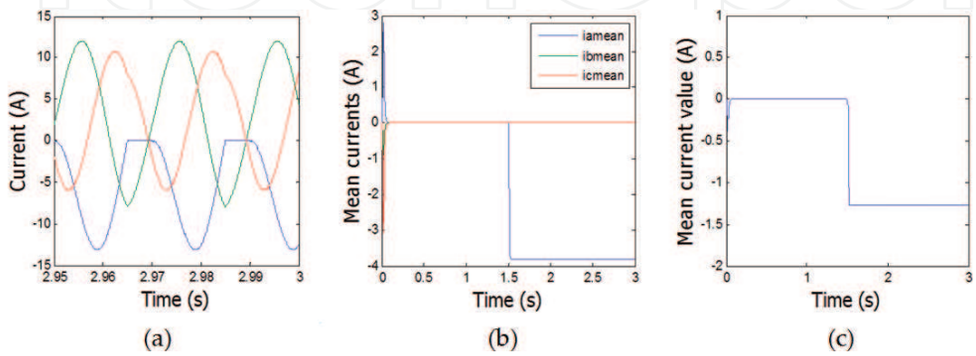

Figure 13. Currents trajectories for a faulty inverter. (a) Three stator currents (I_a, I_b, I_c), (b) Mean values of three stator currents (I_{amean}, I_{bmean}, I_{cmean}), (c) Mean value of current I_{mean}.

4.2. Experimental results for healthy and faulty inverter using the technique of the mean value of the currents

See **Figures 14** and **15**.

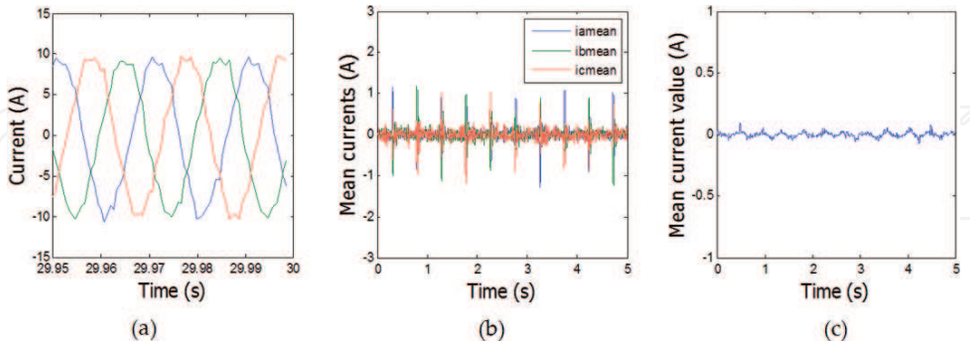

Figure 14. Current characteristics for a healthy inverter. (a) Three stator currents (I_a, I_b, I_c), (b) Mean values of three stator currents (I_{amean}, I_{bmean}, I_{cmean}), (c) Mean value of current I_{mean}.

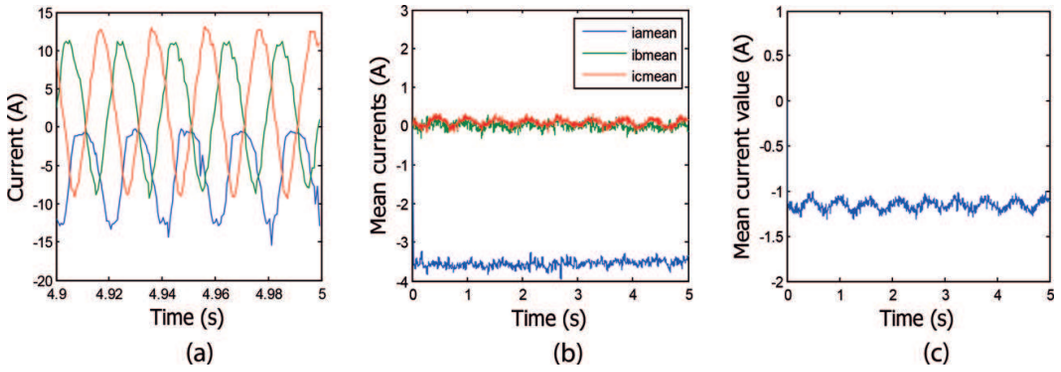

Figure 15. Currents trajectories for a faulty inverter (experimental results). (a) Three stator currents (I_a, I_b, I_c), (b) Mean values of three stator currents (I_{amean}, I_{bmean}, I_{cmean}), (c) Mean value of current I_{mean}.

5. Technique based on the stator current spectrum analysis

This technique is based on the study of the harmonic analysis of each phase current. The amplitude and the argument of each harmonic may be used in the detection and location of the faults [15].

5.1. Simulation results for healthy and faulty inverter using the stator current spectrum analysis

In what follows we will present the simulation for both the healthy state and the inverter with open-circuit switch fault state. **Figure 16** shows the harmonic spectrum of the current for the healthy state.

For an open-circuit K_1 IGBT fault, the harmonic spectrum for each phase is shown as in **Figure 17**. Note that the occurrence of the zero harmonic (i.e., the presence of the DC component) indicates the presence of a fault in K_1.

http://dx.doi.org/10.5772/intechopen.79960

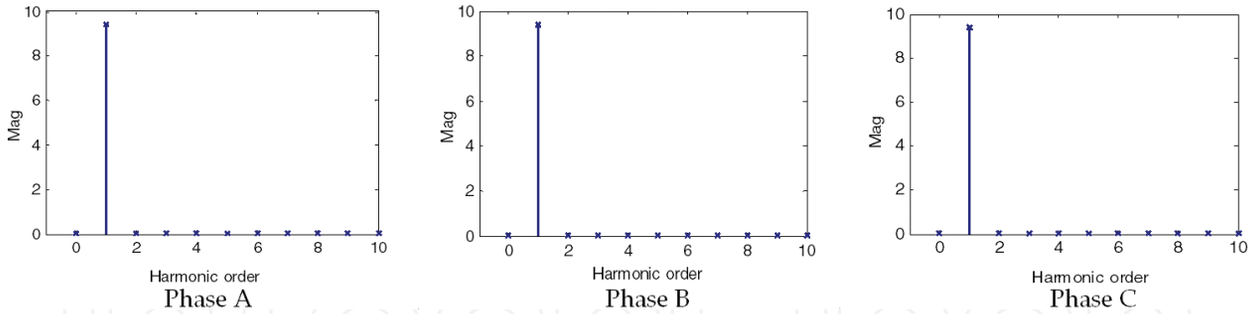

Figure 16. Harmonic spectrum of each phase of a healthy inverter (simulation results).

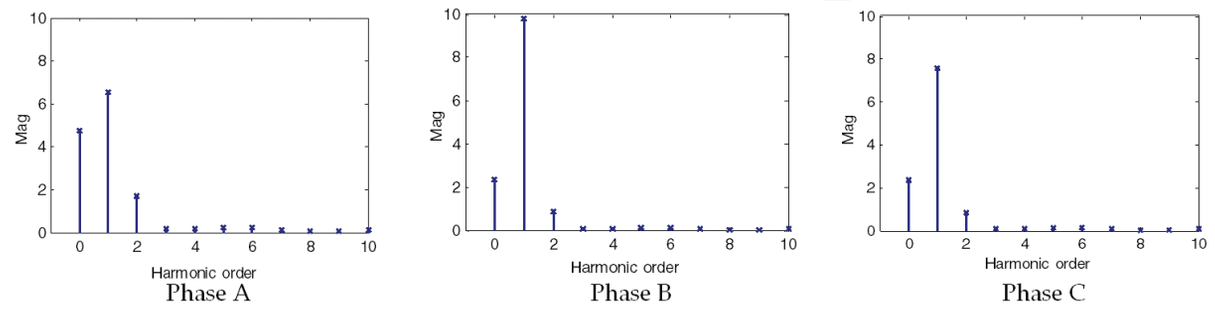

Figure 17. Harmonic spectrum of each phase of a faulty inverter (simulation results).

The analysis of the first eight harmonics shows that the difference between the healthy state and the case of open-circuit fault state lies at the zero-order harmonics which means the presence of the DC component in the signal. The argument of zero harmonic relative to the fundamental enables us to know the type of fault. On the other hand, the argument of this harmonic enables us also to know the faulty switch either the upper one or the lower one.

From the result of **Table 7**, we note that the phase which contains the open-circuit fault has its dc component equals to the sum of the dc component of the two other phases and is expressed by the following relations as:

- If the fault is at phase A, then: $h_{0A} = h_{0B} + h_{0C}$
- If the fault is at phase B, then: $h_{0B} = h_{0A} + h_{0C}$
- If the fault is at phase C, then: $h_{0C} = h_{0A} + h_{0B}$

Where h_{0A} is the zero-order harmonic of phase A, h_{0B} the zero-order harmonic of phase B and h_{0C} the zero-order harmonic of phase C.

5.2. Experimental results for healthy and faulty inverter using the stator current spectrum analysis

In what follows we will present the experimental results for the healthy and open-circuit faulty inverter. **Figure 18** shows the harmonic spectrum of the current for the healthy state, while **Figure 19** depicts the experimental results for open-circuit fault state.

	Zero-order harmonic of the three phases		
Faults types	**Phase A**	**Phase B**	**Phase C**
Healthy case	$\|h_0\| = \varepsilon_{h0}$, $(h_0 = 0)$	$\|h_0\| = \varepsilon_{h0}$, $(h_0 = 0)$	$\|h_0\| = \varepsilon_{h0}$, $(h_0 = 0)$
K_1 *open*	$\varepsilon_{h0} < \|h_0\| < \|h_1\|$ $\varphi_{h0} = 270^0$, $(h_0 = 5.377)$	$\varepsilon_{h0} < \|h_0\| < \|h_1\|$ $\varphi_{h0} = 90^0$, $(h_0 = 2.688)$	$\varepsilon_{h0} < \|h_0\| < \|h_1\|$ $\varphi_{h0} = 90^0$, $(h_0 = 2.688)$
K_2 *open*	$\varepsilon_{h0} < \|h_0\| < \|h_1\|$ $\varphi_{h0} = 90^0 (h_0 = 5.35)$	$\varepsilon_{h0} < \|h_0\| < \|h_1\|$ $\varphi_{h0} = 270^0$, $(h_0 = 2.68)$	$\varepsilon_{h0} < \|h_0\| < \|h_1\|$ $\varphi_{h0} = 270^0$, $(h_0 = 2.68)$
K_3 *open*	$\varepsilon_{h0} < \|h_0\| < \|h_1\|$ $\varphi_{h0} = 90^0$, $(h_0 = 2.68)$	$\varepsilon_{h0} < \|h_0\| < \|h_1\|$ $\varphi_{h0} = 270^0$, $(h_0 = 5.36)$	$\varepsilon_{h0} < \|h_0\| < \|h_1\|$ $\varphi_{h0} = 90^0$, $(h_0 = 2.68)$
K_4 *open*	$\varepsilon_{h0} < \|h_0\| < \|h_1\|$ $\varphi_{h0} = 270^0$, $(h_0 = 2.69)$	$\varepsilon_{h0} < \|h_0\| < \|h_1\|$ $\varphi_{h0} = 90^0$, $(h_0 = 5.39)$	$\varepsilon_{h0} < \|h_0\| < \|h_1\|$ $\varphi_{h0} = 270^0$, $(h_0 = 2.69)$
K_5 *open*	$\varepsilon_{h0} < \|h_0\| < \|h_1\|$ $\varphi_{h0} = 90^0$, $(h_0 = 2.69)$	$\varepsilon_{h0} < \|h_0\| < \|h_1\|$ $\varphi_{h0} = 90^0$, $(h_0 = 2.69)$	$\varepsilon_{h0} < \|h_0\| < \|h_1\|$ $\varphi_{h0} = 270^0$, $(h_0 = 5.38)$
K_6 *open*	$\varepsilon_{h0} < \|h_0\| < \|h_1\|$ $\varphi_{h0} = 270^0$, $(h_0 = 2.69)$	$\varepsilon_{h0} < \|h_0\| < \|h_1\|$ $\varphi_{h0} = 270^0$, $(h_0 = 2.69)$	$\varepsilon_{h0} < \|h_0\| < \|h_1\|$ $\varphi_{h0} = 90^0$, $(h_0 = 5.37)$

Table 7. Open-circuit fault characteristics of an inverter.

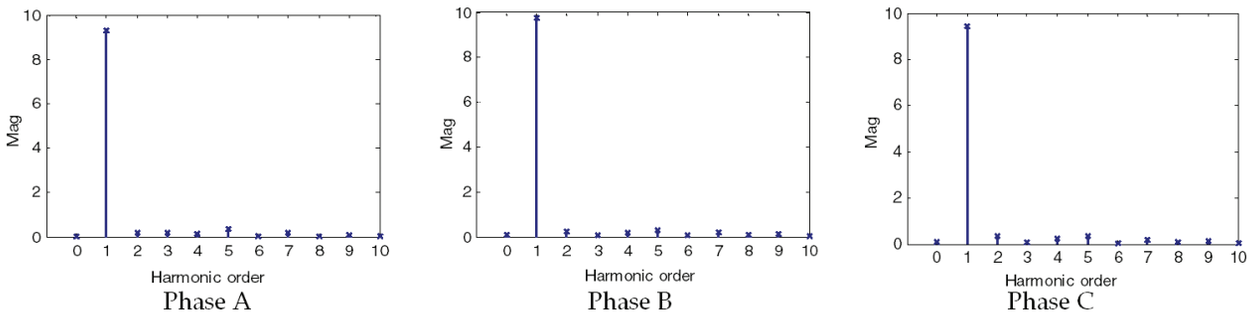

Figure 18. Harmonic spectrum of each phase of a healthy inverter (experimental results).

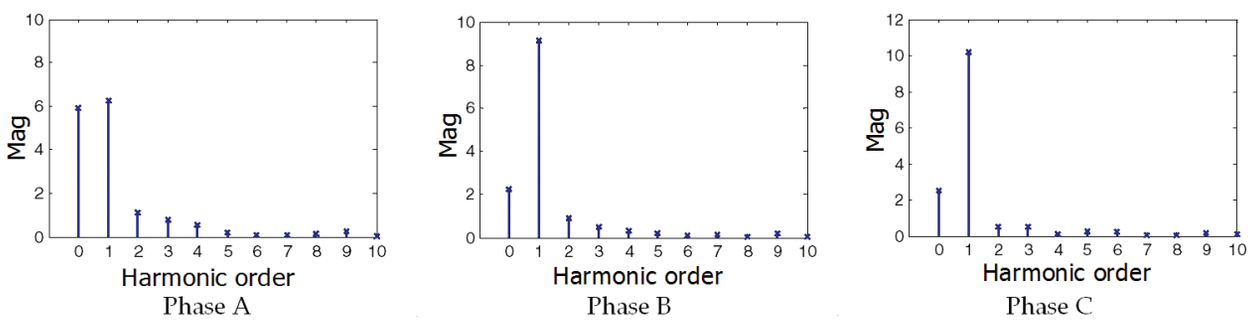

Figure 19. Harmonic spectrum of each phase in case of a faulty inverter (experimental results).

6. Technique based on the measure of the current drop

This technique requires the use of two current sensors by inverter leg. The current measurement may be performed using Hall Effect sensors. Hence the two current sensors for

http://dx.doi.org/10.5772/intechopen.79960

C_{K1}	C_{K2}	$i_{K1} < -i_0$	$i_{K2} < -i_0$	**Conclusion**
1	*0*	*0*	*1*	K_1 open
0	*1*	*1*	*0*	K_2 open

Table 8. Fault detection of a faulty inverter using the measure of the current drop technique.

each leg give the measurements of currents i_{K1} and i_{K2}. If the current of phase A is positive, the K_1 switch is under open-circuit fault if it is ordered to close $C_{K1} = 1$ but the current i_{K2} remains negative. For the K_2 switch and when ik1 is negative, the open-circuit fault is detected if $C_{K2} = 1$ and i_{K1}, remain negative. We therefore obtain the following equations as given in [16]:

$$OC_{K1} = C_{K1}(i_{K2} < -i_0) \tag{12}$$

$$OC_{K2} = C_{K2}(i_{K1} < -i_0) \tag{13}$$

where $C_{K1} = 1$ is the Control of K_1 IGBT and $C_{K2} = 1$ is the Control of K_2 IGBT (**Table 8**).

The algorithm of the open-circuit detection applied in this technique; as shown in **Figure 20**; is based on the measurement of the current drop and can be described by the following steps:

1st step: Measure the current I_j.

2nd step: Search the current error e_j by comparing the current I_j to the threshold current I_0.

3th step: Identify whether any of the six errors exceed the threshold I_0.

4th step: If so, identify the faulty leg of the inverter that should be immediately isolated.

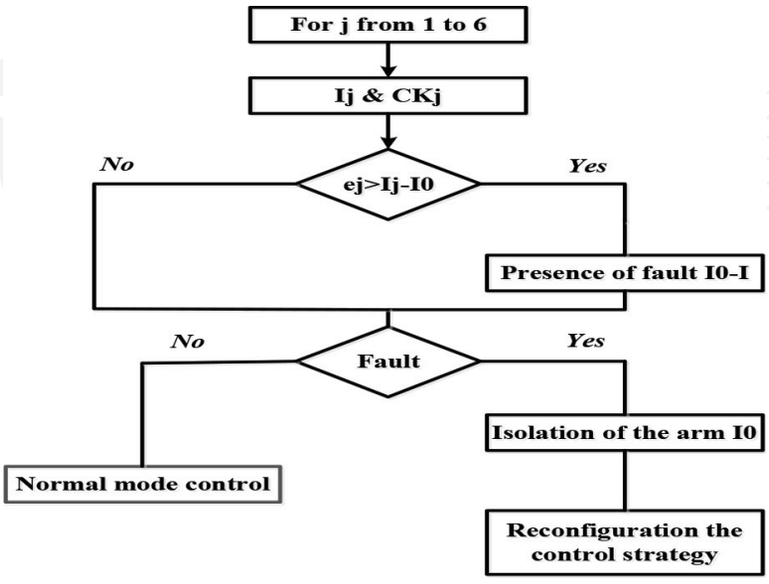

Figure 20. Algorithm for detecting an inverter open-circuit fault using the measure of the current drop.

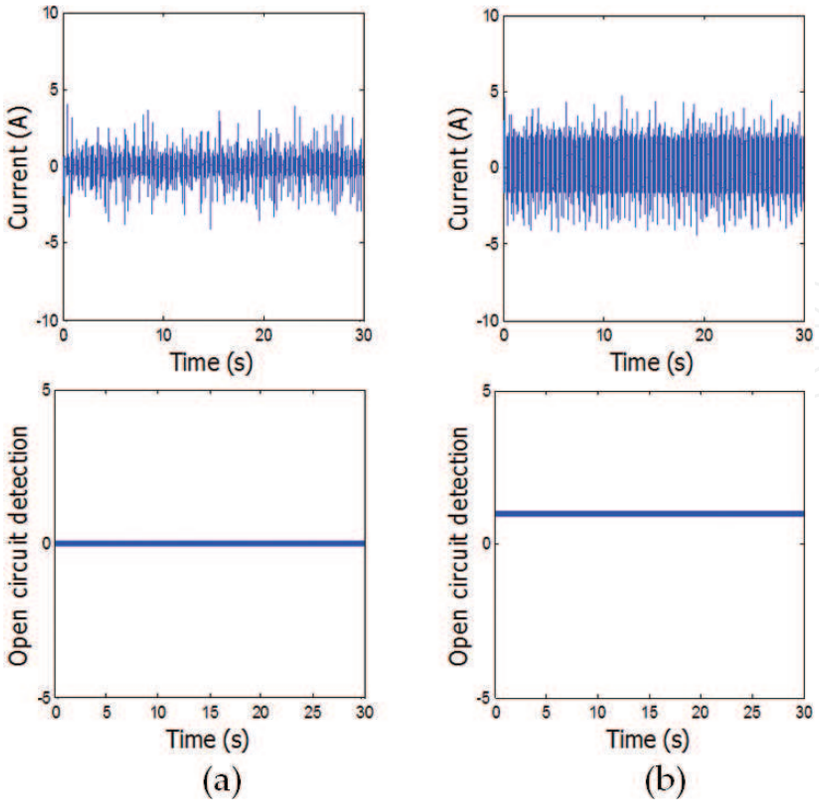

Figure 21. Healthy and faulty inverters detection (a) healthy inverter and (b) open-circuit fault.

In what follows, the experimental results for the case of a healthy inverter state and an open-circuit fault of the K_1 switch state, of an inverter are represented as shown in **Figure 21**, using the technique based on the measurement of the switch current drop.

7. Comparative study between the different techniques

The comparative study is carried out between different detection techniques. The aim of this comparison is to investigate and evaluate the performance of each detection technique studied. The comparison study focuses on the time detection, the localization ability, the hardware aspect and also the error between the threshold set to zero and the fault value. From this comparison study as illustrated both in **Figure 22** and **Table 9**, we come up with the following deductions: the fastest technique in terms of open-circuit fault time detection (*1.5 ms*) is the measurement of the switch current drop technique. Unfortunately this technique presents also two disadvantages: the first one is related to its inability for localization and is used only for detection purpose. The second drawback of this technique is concerned with the hardware and implementation aspect as it utilizes six current sensors (one for each gate of the six IGBT gates of the three phase two-level voltage source inverter).

The three other techniques: the one based on the Park vectors witch polar coordinate, the one based on the average value of the currents and the one based on the current spectral analysis

http://dx.doi.org/10.5772/intechopen.79960

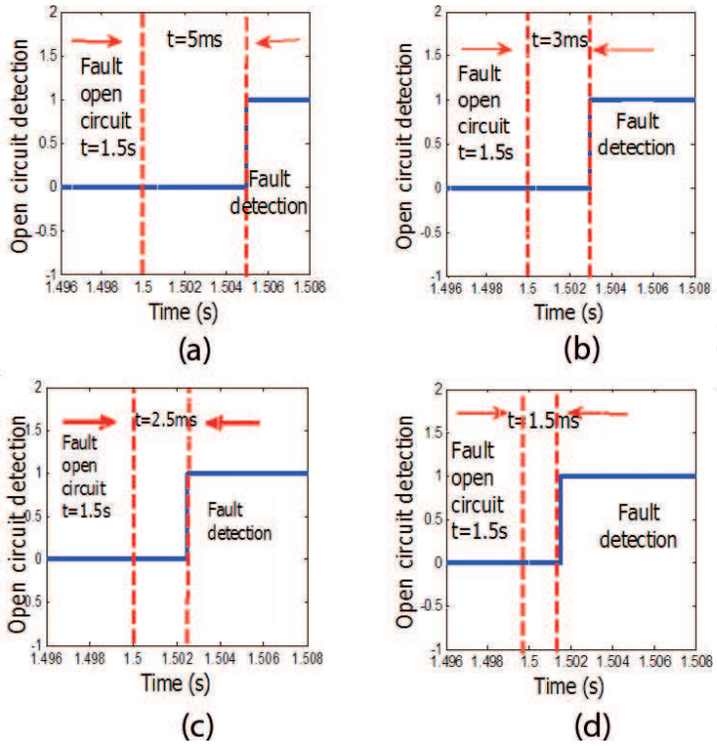

Figure 22. Detection time of open-circuit fault for the four techniques, (a) Park vectors with polar coordinates, (b) mean value of the currents, (c) current spectrum analysis and (d) measure of the current drop.

Techniques	Hardware	Detection time (*ms*)	Detection	Localization	Error	Quality and performance
Park stator current Vectors	Three current sensors	*5*	Yes	Yes	7.62	Good
Average value of stator currents	Three current sensors	*3*	Yes	Yes	1.5	Good
Stator current spectrum analysis	Three current sensors	***2.5***	Yes	Yes	5.37	Very good
Measure of the stator current drop	Six current sensors	*1.5*	Yes	No	3	Average

Table 9. Comparison summary of the detection techniques.

are all used for the detection and localization of open-circuit switch faults in inverters. It should be noted that the three techniques require only three sensors, hence presenting an advantage over the measurement of the current drop technique in terms of cost and implementation. The current spectral analysis has an additional advantage in terms of detection time rapidity (*2.5 ms*) compared to the two other ones (*3* and *5 ms*) respectively. This comparative study is summarized in **Table 9**. For all detection techniques presented in this chapter study, the calculated error in **Table 9**, is that between the normal value corresponding to the threshold for the healthy state case (note that the healthy state is taken as a reference corresponding to zero value of the threshold) relative to the fault value corresponding to the IGBT switch open-circuit fault state.

In what follows, **Figure 22**. illustrates the detection time of the four techniques used for open-circuit fault occurrence at $t = 1.5\ ms$.

8. Conclusion

In this chapter work, the main purpose is to present a very detailed study of some detection techniques using both simulation and experimental work. The study is followed by a performance comparison between the various techniques to illustrate the feasibility and merits of each one of them and shows the suitability of each technique for a diagnostic situation. The study focuses mainly on the detection time as a key parameter in the detection procedure, the ability of the technique to localize in an exact manner the inverter IGBT switch open-circuit fault and also to assess the hardware aspect in terms of number of sensors required. The experimental work is conducted to validate the simulation results obtained.

The Technique based on the measure of the current drop is found to be superior in terms of fault time detection rapidity but unfortunately cannot be used for fault localization which is a drawback with respect to the three other presented techniques. Another disadvantage of this technique is the high number of required current sensors which has doubled in comparison to the three other studied techniques.

The three other techniques based on the Park vectors associated with polar coordinates, the average value of the currents and the current spectral analysis can be all used for detection and localization of inverter IGBT open-circuit faults and they require only three sensors, hence presenting an advantage over the measure of the current drop technique in terms of cost and implementation. The current spectrum analysis has an additional advantage in terms of detection time rapidity (*2.5 ms*) compared to the two other ones (*3 ms* and *5 ms*).

The chapter also proposes polar coordinates calculation to enhance the Park current vectors technic by developing a simple graphical representation which enables the exact computation of both the magnitude and the phase angle of the fault current vector related to the faulty inverter IGBT switch.

Author details

Bilal Djamal Eddine Cherif*, Azeddine Bendiabdellah, Mokhtar Bendjebbar and Laribi Souad

*Address all correspondence to: bilal.cherif@univ-usto.dz

Diagnostic Group, Laboratory LDEE, Electrical Engineering Faculty, University of Sciences and Technology of Oran, Bir El Djir, Algeria

References

[1] Cherif BDE, Bendiabdellah A, Khelif MA. Detection of open-circuit fault in a three-phase voltage inverter fed induction motor. International Review of Automatic Control. 2016; **9**(6):374-382

[2] Eddine CBD, Azzeddine B, Amine KM, Mokhtar B, Noureddine B. The enhancement of park current vectors technique for inverter fault detection. In: Proceedings of the 6th International Conference on Systems and Control; University of Batna 2, Algeria; May 7–9, 2017. pp. 377-382

[3] Orlowska-Kowalska T, Sobanski P. Simple diagnostic technique of a single IGBT open-circuit faults for a SVM-VSI vector controlled induction motor drive. Bulletin of the Polish Academy of Sciences—Technical Sciences. 2015;**63**(1):281-288

[4] Cherif BDE, Bendjebbar M, Benouzza N, Boudinar H, Bendiabdellah A. A comparative study between two open-circuit fault detection and localization techniques in a three phase inverter fed induction motor. In: Proceedings of the 2016 8th International Conference on Modelling, Identification and Control (ICMIC); Algiers; November 2016. pp. 1-7

[5] Zhang W, Xu D, Enjeti PN, Li H, Hawke JT, Krishnamoorthy HS. Survey on fault-tolerant techniques for power electronic converters. IEEE Transactions on Power Electronics. 2014; **29**:6319-6331

[6] Orlowska-Kowalska T, Sobanski P. Simple sensorless diagnosis method for open-switch faults in SVM-VSI-fed induction motor drive. In: IEEE 39th Ann. Conf. of Ind. Electron. Soc.; 2013. pp. 8210-8215

[7] Asghar F, Talha M, Kim SH. Comparative study of three fault diagnostic methods for three phase inverter with induction motor. International Journal of Fuzzy Logic and Intelligent Systems;**17**(4):245-256

[8] Jlassi I, Khojet S, Khil E. A MRAS-Luenberger observer based fault tolerant control of PMSM drive. Journal of Electrical Systems. 2014;**10**(1):48-62

[9] Cherif BDE, Bendjebbar M, Bendiabdellah A. Diagnosis of open-circuit fault in a three phase voltage inverter fed induction motor. In: The 4th International Conference on Electrical Engineering – ICEE'2015; Boumerdes, Algeria

[10] Estima JO, Freire NMA, Cardoso AJM. Recent advances in fault diagnosis by Park's vector approach. IEEE workshop Electr. Mach. Des Control and Diagn. vol. 2. 2013. pp. 279-288

[11] Mendes AMS, Cardoso AJM. Fault diagnosis in a rectifier-inverter system used in variable speed ac drives by the average current Park's vector approach. In: 8th European conference on power electronics and applications, EPE'99. 1999. pp. 1-9

[12] Abramik S, Sleszynski W, Nieznanski J, Piquet HA. Diagnostic method for on-line fault detection and localization in VSI-fed ac drives. In: 10th European Conference on Power Electronics and Applications; Toulouse, France. 2003

[13] Rothenhagen K, Fuchs FW. Performance of diagnosis methods for IGBT open circuit faults in voltage source active rectifiers. In: Proceedings of the .IEEE PESC; 2004. pp. 4348-4354

[14] Cherif BDE, Bendiabdellah A. Detection of two-level inverter open circuit fault using a combined DWT-NN approach, Hindawi. Journal of Control Science and Engineering. Vol. 2018. 11 Pages. Article ID: 1976836

[15] Sharma SK, Lu B. Literature review of IGBT fault diagnostic and protection methods for power inverters. IEEE Transactions on Industry Applications. 2009;**45**(5):1770-1777

[16] Raison B, Rostaing G, Rognon JP. Towards a global monitoring scheme for induction motor drives. In: Int. Power Electron. Conf; Tokyo. 2000. pp. 1183-1188